Received: 21 January 2023 | Revised: 25 February 2023 | Accepted: 27 February 2023

DOI: 10.1111/ter.12647

RESEARCH ARTICLE

Terra Nova WILEY

Earthquake Early Warning System (EEWS) empowered by Time-Dependent Neo-Deterministic Seismic Hazard Assessment (TD-NDSHA)

Yan Zhang[1] | Zhongliang Wu[1,2] | Fabio Romanelli[2,3] | Franco Vaccari[3] | Antonella Peresan[4] | Jiawei Li[5] | Giuliano F. Panza[1,6,7]

[1]Institute of Geophysics, China Earthquake Administration, Beijing, China

[2]Institute of Earthquake Forecasting, China Earthquake Administration, Beijing, China

[3]Department of Mathematics and Geosciences, University of Trieste, Trieste, Italy

[4]National Institute of Oceanography and Applied Geophysics – OGS, Udine, Italy

[5]Institute of Risk Analysis, Prediction and Management (Risks-X), Academy for Advanced Interdisciplinary Studies, Southern University of Science and Technology (SUSTech), Shenzhen, China

[6]Beijing University of Civil Engineering and Architecture (BUCEA), Beijing, China

[7]Associate to the National Institute of Oceanography and Applied Geophysics – OGS, Italy

Correspondence
Zhongliang Wu, Institute of Earthquake Forecasting, China Earthquake Administration, Beijing, China.
Email: wuzl@cea-igp.ac.cn

Fabio Romanelli, Department of Mathematics and Geosciences, University of Trieste, Trieste, Italy.
Email: romanel@units.it

Funding information
National Natural Science Foundation of China, Grant/Award Number: U2039207

Abstract

In the network-based on-site earthquake early warning system (EEWS), the 'blind zone', namely the zone where the issued warning arrives later than the destructive S and surface waves, is one of the challenges affecting its effectiveness. The 'blind zone' is determined by the interstation distance, or equivalently the density of seismic stations, of the network. In this paper, we suggest a practical approach according to which, when in a region a temporary increase of seismic hazard is declared, additional stations are deployed in such a way that the blind zone is temporarily reduced. In the procedure, the time-dependent neo-deterministic seismic hazard assessment (TD-NDSHA) plays a vital role in the identification of the regions potentially exposed to high macroseismic intensities. As a showcase example, we consider the scenario of year 2014 at the Sichuan-Yunnan border of southwest China. The TD-NDSHA is based on the standard NDSHA procedure at regional scale (bedrock conditions), with the 'controlling earthquakes' defined on the basis of the Annual Consultation. We show that the 'blind zone' can be reduced in the identified areas of interest (e.g., MMI ≥ VI), by deploying a limited number of additional seismic stations. In the case where false alarms can be tolerated, significant reduction of the 'blind zone' can be implemented by moving from a network-based EEWS to a single-sensor-based EEWS and skipping the process of location and magnitude-determination/prediction procedures.

KEYWORDS
blind zone, China Seismic Experimental Site, Earthquake Early Warning System (EEWS), time-dependent neo-deterministic seismic hazard assessment (TD-NDSHA)

1 | INTRODUCTION

In the Earthquake Early Warning System (EEWS) scenario considered in this paper, the 'blind zone', defined as the zone within which the warning issue arrives after the destructive S and surface waves, is one of the challenges affecting its effective performance. After an earthquake occurs, the relevant travel time for the destructive S and surface waves is the time needed for these waves to travel from the seismic source to the site(s) of interest. When a seismic network is deployed to issue the early warning, the time needed for the network of seismic sensors to 'sense' the earthquake includes the following: (1) the travel time of P-wave from the seismic source to the sensors, needed for the detection; (2) the time spent to transmit the record of P-waves from the sensor to the data management centre, needed for network processing; (3) the time for the processing of the P-wave records, needed to determine the location and magnitude of the source; and (4) the

time necessary to issue the alarm (Allen & Melgar, 2019). With modern information technology, steps (2) and (4) together can be completed within 1 s. With real-time seismology, step (3) can be completed within 3 s (Allen & Melgar, 2019; Satriano et al., 2011; Wu & Kanamori, 2005). As a rule, steps (2), (3), and (4) can be completed within a total time interval, T_0, of about 4 s (Kuyuk & Allen, 2013). Because of the time needed for the network of seismic sensors to 'sense' the earthquake, steps (1)–(4) in total, it is possible that within a zone centred at the epicentre of the earthquake, the early warning message reaches the target(s) later than the arrival of the S and surface waves. This zone is thus called the 'blind zone' (Kuyuk & Allen, 2013).

The 'blind zone' is mainly dependent on the interstation distance, or equivalently on the density of seismic sensors (see Appendix 1). The ultimate solution to the problem of the 'blind zone' might be a very-dense deployment of seismic sensors. However, in a practical view, this solution is neither operationally convenient nor necessary. In the spatial perspective, it cannot be imagined that for a very large area like China, a very dense seismic network be deployed to 'wait for' a disastrous earthquake with recurrence period of several decades (even several centuries). In the temporal perspective, it is important to notice that seismic networks, as well as the communicating and processing systems, have a limited life time (say 30 years). The worst case might be that the earthquake occurs when the aged system failed to work properly.

One practical solution to this problem, to a large extent not novel, is the following. When in a region a temporary increase of seismic hazard is declared, as in the case of the Annual Consultation on the Likelihood of Earthquakes (Wu, 1997; Zhu & Wu, 2007) or of the areas warned by the M8 or CN algorithms (Peresan et al., 2011), additional stations should be deployed in the relevant areas and thus the 'blind zone' can be temporarily reduced. Evidently the criteria to set up this operation include: (1) the temporary increase of the probability of occurrence of strong earthquakes; (2) the predicted strong ground motion caused by the potential earthquakes; and (3) the population and/or key infrastructures involved. Focusing on the seismological part, we consider here only the first two items, that is, we simply consider the study region as homogeneous in the perspective of exposure. We consider the Sichuan-Yunnan border of southwest China and the hazard scenario of the year 2014 as an example. The inclusion of item 3 requires planned further investigations.

2 | TD-NDSHA FOR EMERGENCY

The output of the intermediate- to short-term earthquake prediction, together with the associated seismic hazard assessment, provides an efficient tool to enhance the effectiveness of EEWS. One of the natural tools for implementing such an assessment is the NDSHA, which has been applied in several places in the last two decades (Panza & Bela, 2019; Bela & Panza, 2021; Panza et al., 2022). As an advanced version of the deterministic seismic hazard assessment, which considers 'controlling earthquakes' or 'scenario earthquakes' as input for seismic hazard assessment (Reiter, 1990), NDSHA convolves a comprehensive physical knowledge of seismic sources, propagation of seismic waves, and their combined interactions with site conditions (Panza et al., 2012, 2022). Compared to traditional siesmic hazard assessments (SHAs) (Probabilistic SHA and/or Deterministic SHA), NDSHA effectively accounts for the tensor nature of earthquake ground motions and does not have to rely on the use of the questionable attenuation relations, that is, the empirical ground motion prediction equations (GMPEs). Last but not least, NDSHA can efficiently handle wave propagation within a three-dimensional media (e.g., La Mura et al., 2011; Gholami et al., 2012, 2013).

In the standard NDSHA computation at regional scale, fully appropriate in the EEWS domain, the synthetic peak ground acceleration (PGA), efficiently computed by modal summation algorithm, is extrapolated to frequencies larger than 1 Hz as follows (Panza et al., 2001; Panza & Bela, 2019): (1) computing synthetic seismograms for $T > 1$ s; (2) matching the normative normalized response spectrum with the long-period portion of the synthetic normalized spectrum and obtain the 'design response spectrum'; and (3) reading the value of the so-obtained 'design response spectra' at $T = 0$ s as the 'Design Ground Acceleration' (DGA).[1] Predicted macroseismic intensity, in terms of the Modified Mercalli Intensity (MMI), is calculated according to the empirical relationship between PGA (or

Significance Statement

Implementation of effective earthquake early warning system (EEWS) may contribute to protecting lives and properties. We show that integrating the information provided by a physically sound, reliable seismic hazard assessment (NDSHA) can significantly improve performances of current EEWS. Specifically, in this study, we demonstrate that EEWS empowered by NDSHA allows reducing the size of 'blind zone', which is one of the challenges affecting performance of these systems. We suggest a practical approach, exploiting information from time-dependent seismic hazard assessment to indicate when and where the number of stations should be temporarily increased. Accordingly, when in a region a temporary increase of seismic hazard is declared (e.g., by Annual Consultation in China Seismic Experimental Site and other validated forecasting tools mentioned in the paper), the corresponding ground-shaking scenarios provided by NDSHA are used to optimally select, based on costs/benefits analysis, the sites where additional stations should be deployed, in such a way that the blind zone could be temporarily reduced. The present work ultimately demonstrates how basic studies in earthquake science, including studies on the physics of seismic-waves propagation and the knowledge of the Earth's interior, could contribute directly to the engineering endeavour towards reduction of seismic disaster risk.

DGA) and MMI (Wald et al., 1999). In practice, MMI can be regarded as a good approximation of the Chinese intensity scale (Chen & Booth, 2011). For EEWS, the critical regions are those with intensity above VI, which indicates the areas prone to destruction and delimits the 'seismic disastrous regions'.

For the region of the China Seismic Experimental Site (CSES), and for the year 2014, we demonstrated that the Annual Consultation-based TD-NDSHA properly describes the seismic hazard as compared to the actual earthquakes, as evaluated by confusion matrix and Molchan error diagram (Molchan, 1997; Zhang et al., 2022).

3 | A SCENARIO OF THE SICHUAN-YUNNAN BORDER, YEAR 2014

We consider the Sichuan-Yunnan border of southwest China and the hazard scenario of the year 2014 as an example. NDSHA maps were produced for a larger geographical domain: the CSES and its surrounding areas (Zhang, Romanelli, et al., 2021). The study region is located in the northeastern part of CSES (see Figure 1)

Procedures of the TD-NDSHA for earthquake emergency are described by the flow chart given in Appendix 2 (Figure A1). We use a dataset and procedures similar to that described by Zhang, Romanelli et al. (2021), but as 'controlling earthquakes' or 'scenario earthquakes' we consider those defined by the Annual Consultation for the year 2014, organized by the China Earthquake Administration (CEA) at the end of 2013.[2] The alerted region for seismic hazard at annual scale, as shown in Figure 1, was determined by a multidisciplinary approach in which experts' opinions played an important role (e.g., Wu, 1997; Zhu & Wu, 2007). The expected magnitude of earthquakes was ~7; hence it is natural to consider the magnitude 7.0±0.5, where 0.5 corresponds to twice the global standard error of magnitude estimate (0.2–0.3) as per Båth (1973) and Bormann et al. (2007). Within this region, two strong earthquakes occurred in 2014[3], 3 August Zhaotong earthquake (M_S6.5, M_W6.2), and 22 November Kangding earthquake (M_S6.3, M_W5.9). In the latter hazard computation, we use surface magnitude (M_S) as input for the consistency with the *Open File of the Annual Consultation on the Likelihood of Earthquakes for the Year 2014*, subject to the Panel Discussion in the Annual Consultation Meeting[2]. Actually, these are magnitude 6.8 and 6.5, respectively, earthquakes according to presumably final CENC database, which appears as a favourable fit of the expected magnitude (7.0±0.5) defined by the Annual Consultation for the year 2014. It should be noted that according to the USGS these events are M_W6.2–33 km WSW from Zhaotong, China (2014-08-03 08:30:13 UTC, 27.189°N, 103.409°E, 12.0 km depth[4]), M_W5.9–37 km NW from Kangding, Western Sichuan, China (2014-11-22 08:55:26 UTC, 30.340°N,101.737°E, 9.0 km depth[5]), respectively. The Kangding's aftershock M_W5.6 (2014-11-25 15:19:08 UTC, 30.188°N,101.762°E, 9.0 km depth[6]) impact on already destabilized constructions was, perhaps, comparable or even more destructive than that of the main shock (according to PAGER both quakes produced I_{MMI} = IV at Kangding with population of 100k[5,6]). This implies that such intermediate-term medium-range earthquake prediction has sound scientific basis and is useful in practice. Statistical evaluation shows that such annual prediction outperforms random guess, albeit to a large extent depending on the analysis of seismicity (e.g., Shi et al., 2001; Zhang et al., 2002).

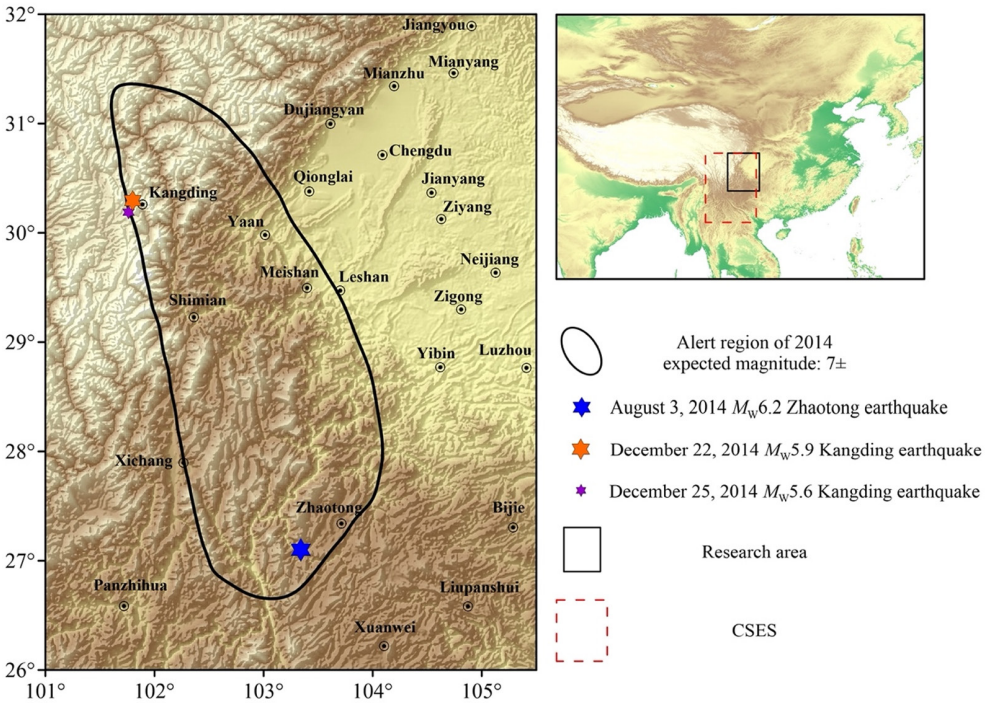

FIGURE 1 Alert region with expected magnitude 'about 7' identified by the Annual Consultation for the year 2014, with August 3, M_W6.2 Zhaotong earthquake, and December 22, M_W5.9 Kangding earthquake together with its M_W5.6 aftershock on December 25, occurred in 2014. [Colour figure can be viewed at wileyonlinelibrary.com]

The input for the 'controlling earthquakes' or 'scenario earthquakes' considers the 'expected earthquakes' defined by the Annual Consultation, with magnitude 7.0. The depths of these 'scenario earthquakes', located at the centre of the predefined grids of size 0.2° ×0.2° within the alert region of the Annual Consultation, are taken as 15 km according to the statistics of local seismicity. Focal mechanism of the 'scenario earthquakes' (Strike = 20°, Dip = 46°, Rake = 72°) is based on the data of historical earthquakes. Figures 2 and 3 shows the predicted maximum horizontal ground acceleration, in terms of the Design Ground Acceleration (DGA), and the deduced macroseismic intensity (MMI). Within the areas with intensity higher than VI, the EEWS is considered.

Prediction of ground shaking intensities is made considering the same parameter setting as that of Zhang, Romanelli et al. (2021), in which a piece-wise 1-D velocity model is used. In search of simplicity, it is natural to use a homogeneous half-space structural model, whose velocity is given by the average of the piece-wise 1-D model: $V_S = 3.4$ km/s, $V_P = 5.9$ km/s. The depth of the scenario earthquakes is taken as 15 km, identical to that used in the TD-NDSHA (Zhang et al., 2022).

4 | MODE-SWITCHING STRATEGY FOR EEWS

For the reduction of 'blind zone', we propose two of the ingredients for the decision-making, i.e. Mode-Switching Strategy for EEWS: (1) the increased probability of earthquakes as defined by the Annual Consultation, and (2) the estimated seismic hazard as implemented by TD-NDSHA. Although not discussed in detail, the involved regions (taken as homogeneous as far as exposures are concerned) are characterized by dense population (as can be seen from the distribution of cities in Figure 1) and key infrastructures (such as major plants/reservoirs and/or railways/highways/pipelines), in which EEWS plays an important preventive role in protecting lives and properties.

The extent of the 'blind zone' is determined by the distribution of seismic sensors. Figure 4 shows the map of interstation distance defined as the average distance between the three closest stations: the closest, the 2nd closest, and the 3rd closest (Kuyuk & Allen, 2013). The seismograph stations belong to either the national or the provincial earthquake monitoring systems, with data collected by the China Earthquake Networks Center (CENC), and strong motion stations with data collected by the China Strong Motion Network Center (CSMNC). These stations can now be used for earthquake early warning, but at the time of the 2014 scenario case, no EEWS was operating in the study area. The distribution of stations also determines, for any place to be considered, the distance to the 1st, the 2nd, the 3rd, ..., and the 7th closest station, respectively, which can be used to estimate the size of the blind zone (Kuyuk & Allen, 2013; see Appendix 1). Figures 5–8 maps the size of the 'blind zone' using

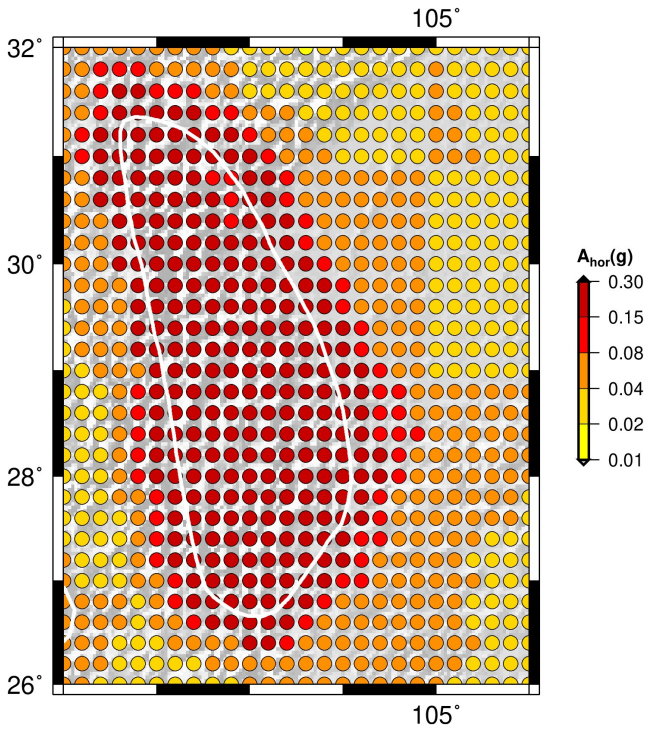

FIGURE 2 TD-NDSHA predicted maximum horizontal acceleration in terms of Design Ground Acceleration (DGA). White irregular contour indicates the alert region identified by the Annual Consultation for the year 2014. [Colour figure can be viewed at wileyonlinelibrary.com]

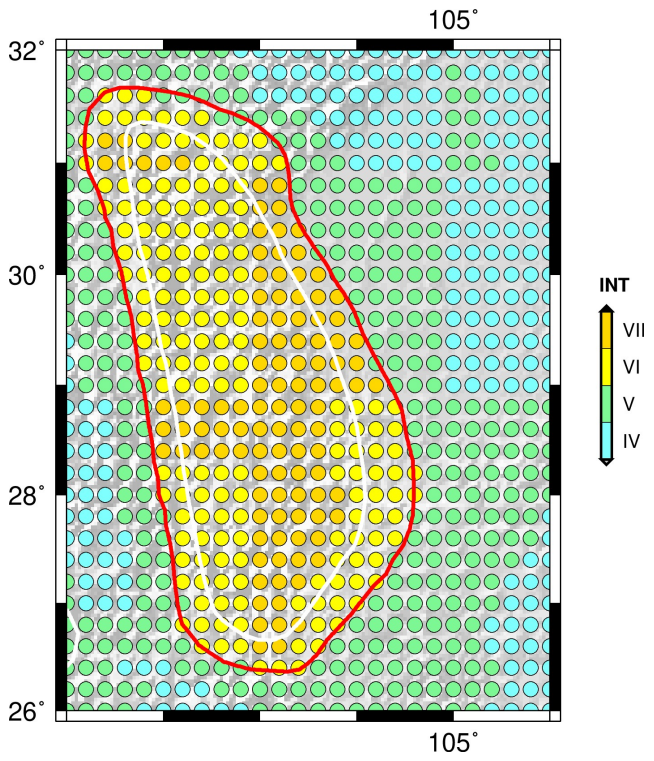

FIGURE 3 Predicted macroseismic intensity (INT, in MMI scale) calculated from the predicted ground motion parameters shown in Figure 2. White irregular contour indicates the alert region identified by the Annual Consultation for the year 2014. The red irregular line delineates the area where MMI ≥ VI. [Colour figure can be viewed at wileyonlinelibrary.com]

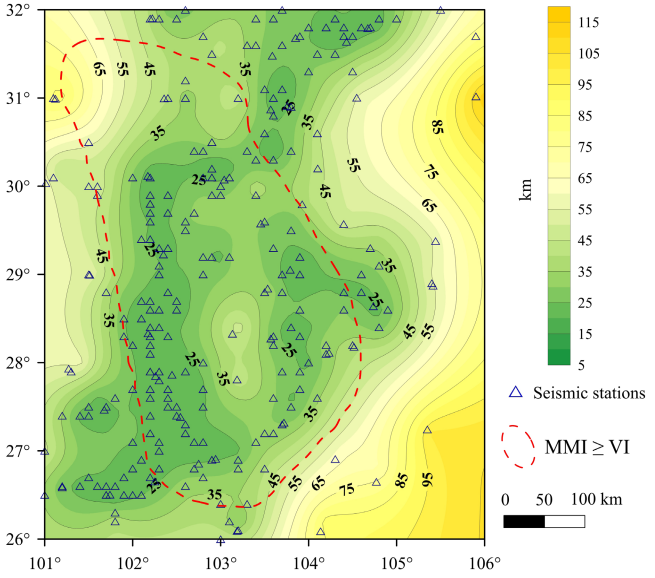

FIGURE 4 Area with predicted intensity MMI ≥ VI, based on the Annual Consultation and TD-NDSHA, with map of interstation distance defined as the average distance to the three closest stations (Kuyuk & Allen, 2013). The interstation distance is mapped by the isolines with Krigging interpolation. The stations (till 2018) include seismic stations with data collected by the China Earthquake Networks Center (CENC) and strong motion stations with data collected by the China Strong Motion Network Center (CSMNC). [Colour figure can be viewed at wileyonlinelibrary.com]

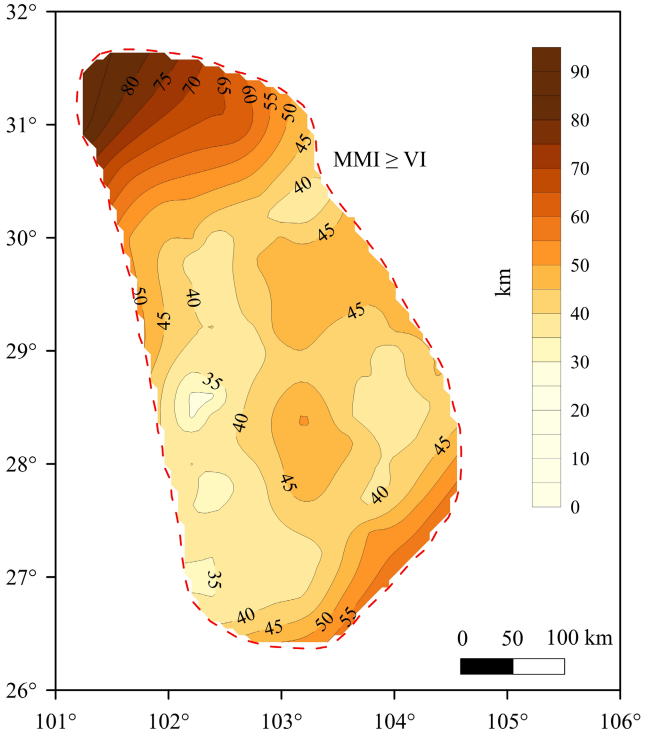

FIGURE 5 Map of the size, in km, of the 'blind zone' when a 7-station triggering criterion is used. [Colour figure can be viewed at wileyonlinelibrary.com]

a 7-station, 6-station, 5-station and 4-station, triggering criteria, respectively. It can be seen that by decreasing the number of stations required to identify a P-wave arrival in the alert algorithm, the size of the blind zone decreases accordingly. Meanwhile, for the same triggering mode, the smaller the interstation distance, the smaller is the size of the 'blind zone', as can be seen from the difference from place to place.

Figures 4– 8 suggest the following switch on strategy to improve the EEWS by reducing the size of the 'blind zone':

- *The 'professional'* strategy: increase the number of stations, or equivalently decrease the interstation distance. This can be clearly seen in Figures 4 and 6 (the 6-station triggering mode). In Figure 6, the size of the 'blind zone' is different for different places. In the northern part of the intensity VI area, the size of the 'blind zone' is up to 80 km, where the interstation distance is about 65 km. In contrast, in the mid-west part, the size of the 'blind zone' is about 40 km, where the interstation distance is some 20 km. This rough comparison simply suggests that to decrease the interstation distance by increasing the density of seismic sensors may effectively decrease the size of the 'blind zone'. The quantitative relationship between the size of the 'blind zone' and the interstation distance is well depicted in Figure 9, which extends the result of Kuyuk and Allen (2013) from 1–4 stations to 4–7 stations. In Figure 9 the parameters used are the ones given for the study region by Zhang, Romanelli et al. (2021), which are different from those used for southern California (Kuyuk & Allen, 2013). In the figure, it can be seen that if the interstation distance decreases, for example, in 7-station triggering mode, from 30 km (point A) to 20 km (point B), then the size of the 'blind zone' may decrease from about 44 km (point D) to about 33 km (point C).
- *The 'public' strategy* : change from network-based EEW to single-sensor-based EEW, skipping the process of the location and magnitude-determination/prediction procedure. The location and magnitude-determination/prediction procedure, which takes T_0 ~ 4 s, plays an important role in contributing to the forming of the 'blind zone': minimizing T_0 reduces the 'blind zone'. Figure 10 shows the scenario of an extreme case when T_0 equals zero, and only one station is used for the alarm. That is, when the sensor (not necessarily professional seismic or strong motion sensor, mostly Micro Electro-Mechanical Systems (MEMS)-based acceleration sensors, see Wu et al., 2019) detects the ground motion above a given threshold, it issues the alarm to the end user. This may cause significant false alarms. But for cases like an ophthalmic surgery, the negative effect of the false alarm is small, and the positive effect of the warning is critical. A possible scenario of this case is: the EEWS issues an alarm, and the surgeon suspends the operation for a moment, taking the (laser) scalpel from the eye of the patient; if the alarm is a false alarm, the doctor simply continues the operation, otherwise, if the alarm is not declared, but the seismic ground motion is severe, the surgery disturbed by

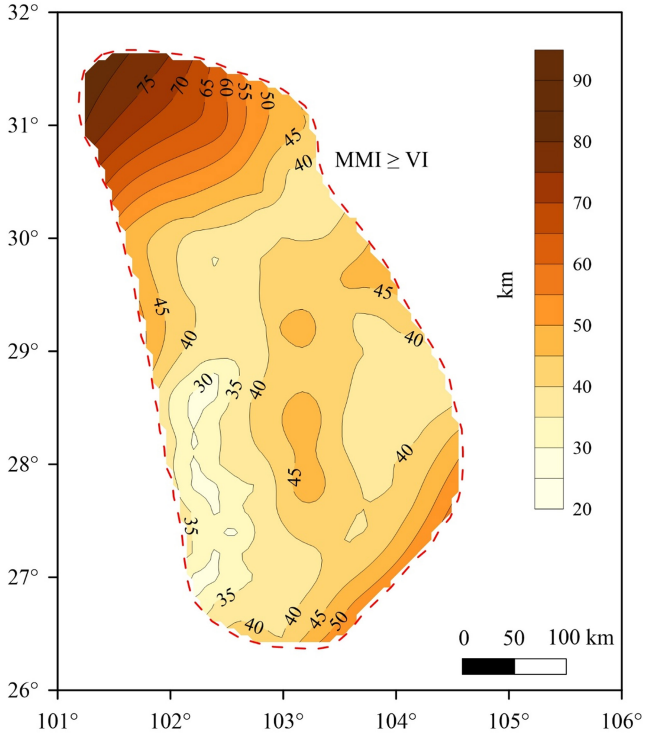

FIGURE 6 Map of the size, in km, of the 'blind zone' when a 6-station triggering criterion is used. [Colour figure can be viewed at wileyonlinelibrary.com]

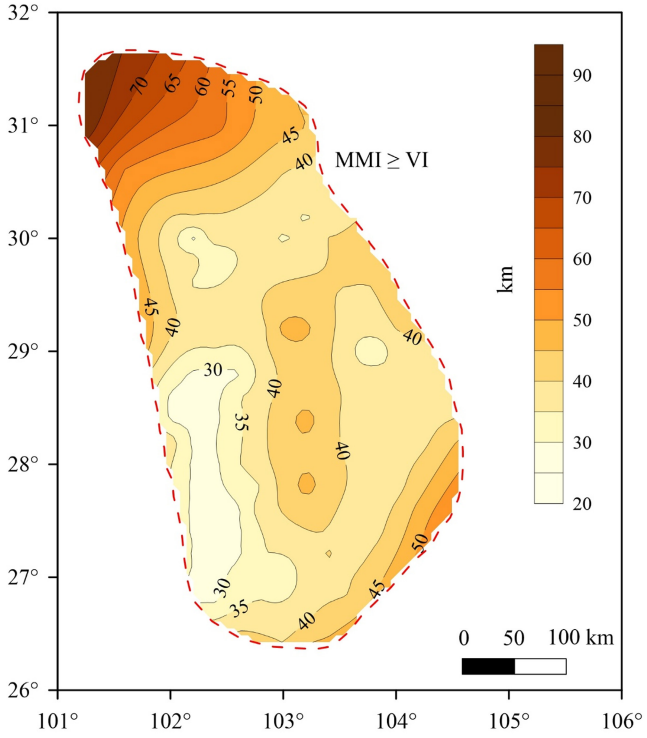

FIGURE 7 Map of the size, in km, of the 'blind zone' when a 5-station triggering criterion is used. [Colour figure can be viewed at wileyonlinelibrary.com]

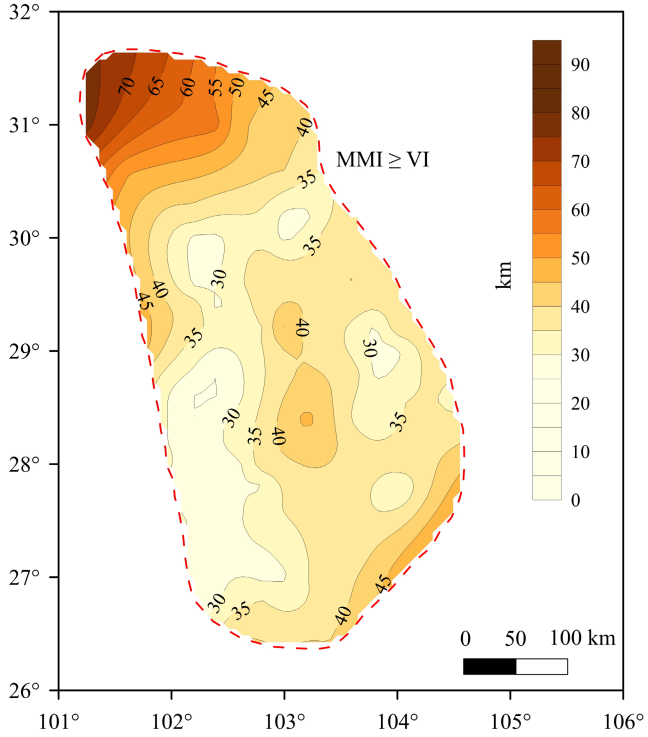

FIGURE 8 Map of the size of the 'blind zone' when a 4-station triggering criterion is used. [Colour figure can be viewed at wileyonlinelibrary.com]

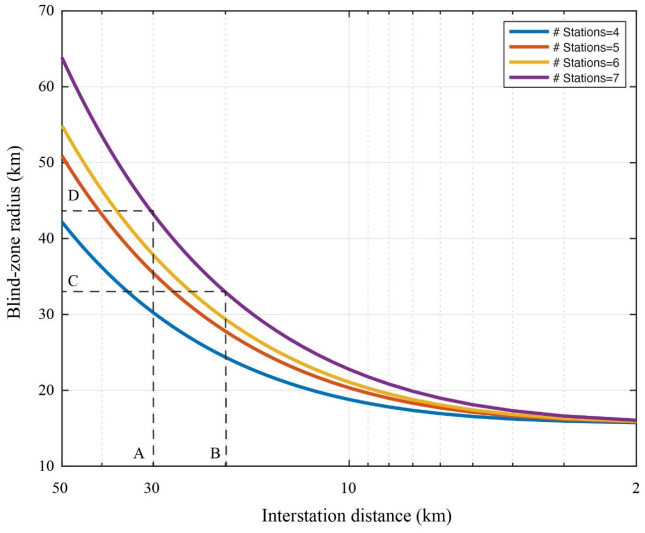

FIGURE 9 Relationship between the size of the 'blind zone' and interstation distance with respect to the number of stations needed to identify the first P-wave arrival. The figure reproduces the curves of Kuyuk and Allen (2013), with parameters V_s 3.4 km/s, V_p 5.9 km/s, and focal depth 15 km. The figure is convenient for the analysis of the relation between the size of the 'blind zone' (vertical axis) and the interstation distance (horizontal axis). For example, in the case that 7 stations are required in the location and magnitude determination/prediction (the line in purple), if the interstation distance decreases from point A (30 km) to B (20 km), then the size of the 'blind zone' may decrease from point D (~44 km) to C (~33 km). [Colour figure can be viewed at wileyonlinelibrary.com]

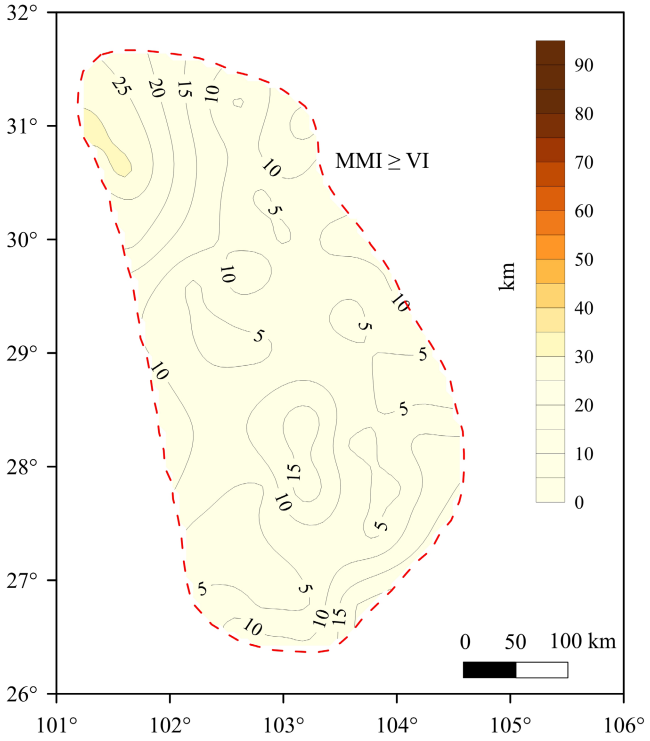

FIGURE 10 Map of the size of the 'blind zone' when a 1-station triggering criterion is used and the time required by the procedure of location and magnitude determination/prediction is neglected. [Colour figure can be viewed at wileyonlinelibrary.com]

the strong ground motion could cause unthinkable tragedies. In general, tolerance of possible errors, including missed warnings and false alarms (both implying some related costs) depends on the features of the targets to be protected, which needs a sophisticated and considerate design of the end-user service (e.g. Molchan, 1997).

- *The 'professional–public' strategy*: from the perspective of the '*professional*' strategy, and the perspective of the '*public*' strategy, the competitive point is the choice between professional seismic stations and low-cost sensors. Wu et al. (2013) developed a P-wave alert device based on MEMS accelerometers, *P* alert. It was designed to send warning alarm once an earthquake is detected by any of the sensors. Compared to professional seismic station, in the procedures of earthquake early warning, MEMS-based acceleration sensors care about the arrival of P-wave and the issue of alarm, i.e., step (1) the travel time of P-wave from the seismic source to the sensors, needed for the detection, and step (4) the time necessary to issue the warning, but professional seismic station cares about all steps, albeit with larger 'blind zone'. If professional stations and MEMS-based acceleration sensors are deployed on a large scale in the region with higher seismic risk in the meantime, in other words, both the professional and public strategies are applied, the uncertainties and size of 'blind zone' may be simultaneously decreased. Indeed, for such a large-scale deployment, the results of SHA play an essential role in determining where to set up the different sensors.

It is worth noting that both the '*professional*' and '*public*' strategies are useful for the seismic protection of different objects. Determining which one is preferable depends on the properties of protected targets, for which some standard criteria may be quantitatively proposed to support the decision process (e.g., Molchan, 1997). For constructing such standard criteria, false and missed alarms rates need to be assessed and they should be considered for properly balancing tolerance and return. For instance, a *matrix* can be built in which false and missed alarm rates are distributed in rows, cost and return are in columns, and standard criteria depend on their *tradeoff*. Indeed, that is a kind of question of Nash Equilibrium in Game theory,[7] and the answer is up to *the* scenario. Occasionally, it is required to implement both the '*public*' and '*professional*' strategies in the same region. In 2015, the CEA launched a demonstration EEW project by constructing EEWS in three test regions, i.e., the Beijing-Tianjin-Hebei region, the Fujian costal area, and the Sichuan-Yunnan border region, where traditional seismic stations and low-cost sensors coexist (Peng et al., 2020). The authors focused on the Sichuan-Yunnan border region, finding that the average reporting time for M_L 4.0+ earthquakes was reduced to ~9 s.

5 | CONCLUSIONS AND DISCUSSION

Earthquake early warning system makes use of the message carried by the P-wave arrival to issue warnings about the later coming, and potentially destructive, S and surface waves, to field emergency countermeasures, which are scaled to the different objects to be protected (Allen et al., 2009; Allen & Melgar, 2019; Cremen et al., 2022; Kanamori, 2005; Satriano et al., 2011). If the detection network does not cover the seismic source, it has been shown that SHA may help to improve their performance (Cremen & Galasso, 2020; Zhang, Wu et al., 2021). In this paper we focus on the case that the network covers both the seismic source and the target to be protected, and explore how TD-NDSHA, (see Panza et al., 2022) may help. In general, it is not cost-efficient to maintain a seismic network with dense stations deployed for a long time. The gradual aging of equipment will also produce much more uncertainties. Accordingly, to increase the number of stations in the region with potentially higher seismic hazard will be a significant option. For such a realistic demand, TD-NDSHA might be a good candidate for a 'standard tool', indeed TD-NDSHA might be wrong, as all models, but it could be really useful (Kossobokov & Panza, 2022) for the EEWS purpose considered here.

In this paper, we use a scenario case of the year 2014 for the Sichuan-Yunnan border of southwest China to illustrate such a concept. We consider the network-based on-site EEWS, in which the 'blind zone' is a major challenge affecting the effectiveness of EEWS. The Annual Consultation on the Likelihood of Earthquakes and the associated NDSHA provide the EEWS with the distribution of predicted ground motion parameters and expected intensities at one-year time scale. The reduction of the size of the 'blind zone' can be conducted by switching the mode of EEW at two levels, namely (1) increase of the number of stations, or equivalently decrease of the

interstation distance; and (2) for regions and cases in which false-alarms can be tolerated to much extent, change from network-based EEW to single-sensor-based EEW, skipping the process of the location and magnitude-determination/prediction procedure.

In the TD-NDSHA practice, it must be noted that the important component is SHA, especially TD. ND plays a crucial role in the computation of SHA, in which the realization of TD is indeed a challenge. As a development of NDSHA, TD is gradually being a part of NDSHA, with the important development of introducing intermediate-term medium-range earthquake prediction results from other methodologies (Keilis-Borok & Soloviev, 2003). In this context, there have been a lot of significant experiments, for example, M8, CN (Panza et al., 2022). In this paper, we discuss another possibility, the Annual Consultation. Here the Annual Consultation plays the role of intermediate-term medium-range earthquake prediction. Other approaches, such as the M8 or CN algorithms (e.g., Peresan et al., 2011), to the identification of increased probability of earthquakes can be readily used as well to supply a more complete picture of the impending hazard. For the seismic hazard assessment, which is associated to the areas with temporary increased probability of earthquakes, NDSHA is, so far, the most suitable algorithm to be used, because of its consideration of comprehensive physical knowledge of seismic sources, propagation of seismic waves, and their combined interactions with site conditions. Meanwhile, as a key ingredient of NDSHA, ND is being upgraded in terms of wave propagation in three-dimensional heterogeneous media (La Mura et al., 2011; Gholami et al., 2013).

In the EEW practice, the more the number of stations in the location and magnitude determination/prediction procedure are used, the higher is the quality of the parameter estimate, as tested in the operations of some prototype EEWS (e.g., Peng et al., 2011). As an extreme case, the 'public strategy' has significant risks associated with its uncertainty and instability. To compensate such uncertainties and risks, one of the measures to be considered is to conduct the mode-switching and the regular EEW operation in parallel. The regular EEWS uses enough stations in the location and magnitude determination/prediction and thus can be used as a 'ground truth' (i.e. a reference), albeit with larger blind zone. In this case, the regular EEW may correct the mistake/error, even if late in time. In the case of failures to detect, this does not help, but in the case of false alarms, it helps much. A scenario of the latter case is that within the 'blind zone' the system issues an alarm, but 1 s later the regular EEWS issues that the magnitude is not as large as first reported, and the alarm is thus cancelled.

ACKNOWLEDGEMENTS

This work is supported by the National Natural Science Foundation of China (NSFC, grant number U2039207). We thank two anonymous reviewers for their help in improving and polishing the manuscript.

CONFLICT OF INTEREST STATEMENT

The authors declare that they have no known competing financial interests or personal relationships that could have appeared to influence the work reported in this paper.

DATA AVAILABILITY STATEMENT

Data sharing not applicable to this article as no datasets were generated or analysed during the current study.

ENDNOTES

[1] Incidentally, we observe that the extrapolation is not needed to obtain PGV and PGD since, as a rule, they correspond to $T \geq 1$ s.

[2] China Earthquake Networks Center (CENC) eds., 2013. *Open File of the Annual Consultation on the Likelihood of Earthquakes for the Year 2014*, subject to the Panel Discussion in the Annual Consultation Meeting. Beijing: China Earthquake Administration, in Chinese.

[3] Magnitude published by the China Earthquake Networks Center (CENC) in its quick earthquake determination (QED) report.

[4] https://earthquake.usgs.gov/earthquakes/eventpage/usb000rzmg/executive. Last accessed on February 13, 2023.

[5] https://earthquake.usgs.gov/earthquakes/eventpage/usb000syy0/executive. Last accessed on February 13, 2023.

[6] https://earthquake.usgs.gov/earthquakes/eventpage/usb000szw2/executive. Last access on February 13, 2023.

[7] Tadelis, S., 2013. *Game Theory: An introduction*. New Jersey: Princeton University Press.

REFERENCES

Allen, R. M., Gasparini, P., Kamigaichi, O., & Böse, M. (2009). The status of earthquake early warning around the world: An introductory overview. *Seismological Research Letters*, *80*, 682–693. https://doi.org/10.1785/gssrl.80.5.682

Allen, R. M., & Melgar, D. (2019). Earthquake early warning: Advances, scientific challenges, and societal needs. *Annual Review of Earth and Planetary Sciences*, *47*, 361–388. https://doi.org/10.1146/annurev-earth-053018-060457

Båth, M. (1973). *Introduction to seismology*. Birkhäuser Verlag.

Bela, J., & Panza, G. F. (2021). NDSHA - the new paradigm for RSHA - an updated review. *Vietnam Journal of Earth Sciences*, *43*, 111–190. https://doi.org/10.15625/2615-9783/15925

Bormann, P., Liu, R. F., Ren, X., Gutdeutsch, R., Kaiser, D., & Castellaro, S. (2007). Chinese National Network magnitudes, their relation to NEIC magnitudes, and recommendations for new IASPEI magnitude standards. *Bulletin of the Seismological Society of America*, *97*, 114–127. https://doi.org/10.1785/0120060078

Chen, Y., & Booth, D. (2011). *The Wenchuan earthquake of 2008: Anatomy of a disaster*. Scientific Press/Springer.

Cremen, G., & Galasso, C. (2020). Earthquake early warning: Recent advances and perspective. *Earth-Science Reviews*, *205*, 103184. https://doi.org/10.1016/j.earscirev.2020.103184

Cremen, G., Galasso, C., & Zuccolo, E. (2022). Investigating the potential effectiveness of earthquake early warning across Europe. *Nature Communications*, *13*, 639. https://doi.org/10.1038/s41467-021-27807-2

Gholami, V., Hamzehloo, H., La Mura, C., Ghayamghamian, M. R., & Panza, G. F. (2013). Simulation of selected strong motion records of the 2003 Mw=6.6 bam earthquake (SE Iran), the modal summation-ray tracing methods in the WKBJ approximation. *Geophysical Journal International*, *196*, 924–938. https://doi.org/10.1093/gji/ggt405

Gholami, V., La Mura, C., Hamzehloo, H., & Panza, G. F. (2012). *3-dimensional modal summation simulation of 2003 Mw=6.6 bam earthquake south Estern Iran* (pp. 3418–3427). 15th world conference on earthquake engineering 2012 (15WCEE).

Kanamori, H. (2005). Real-time seismology and earthquake damage mitigation. *Annual Review of Earth and Planetary Sciences*, *33*, 195–214. https://doi.org/10.1146/annurev.earth.33.092203.122626

Keilis-Borok, V. I., & Soloviev, A. A. (2003). *Nonlinear dynamics of the lithosphere and earthquake prediction*. Springer.

Kossobokov, V., & Panza, G. (2022). Seismic roulette: Hazards and risks. *Terra Nova*, *34*, 475–494. https://doi.org/10.1111/ter.12617

Kuyuk, H. S., & Allen, R. M. (2013). Optimal seismic network density for earthquake early warning: A case study from California. *Seismological Research Letters*, *84*, 946–954. https://doi.org/10.1785/0220130043

La Mura, C., Yanovskaya, T. B., Romanelli, F., & Panza, G. F. (2011). Three-dimensional seismic wave propagation by modal summation: Method and validation. *Pure and Applied Geophysics*, *168*, 201–216. https://doi.org/10.1007/s00024-010-0165-2

Molchan, G. M. (1997). Earthquake prediction as a decision-making problem. *Pure and Applied Geophysics*, *149*, 233–247.

Panza, G. F., & Bela, J. (2019). NDSHA: A new paradigm for reliable seismic hazard assessment. *Engineering Geology*, *275*, 105403. https://doi.org/10.1016/j.enggeo.2019.105403

Panza, G. F., Kossobokov, V. G., Laor, E., & De Vivo, B. (Eds.). (2022). *Earthquakes and sustainable infrastructure: Neodeterministic [NDSHA] approach guarantees prevention rather than cure*. Elsevier.

Panza, G. F., La Mura, C., Peresan, A., Romanelli, F., & Vaccari, F. (2012). Seismic hazard scenarios as preventive tools for a disaster resilient society. *Advances in Geophysics*, *53*, 93–165. https://doi.org/10.1016/B978-0-12-380938-4.00003-3

Panza, G. F., Romanelli, F., & Vaccari, F. (2001). Seismic wave propagation in laterally. Heterogeneous anelastic media: Theory and application to seismic zonation. *Advances in Geophysics*, *43*, 1–95. https://doi.org/10.1016/S0065-2687(01)80002-9

Peng, C. Y., Ma, Q., Jiang, P., Huang, W. H., Yang, D. K., Peng, H. S., Chen, L., & Yang, J. S. (2020). Performance of a hybrid demonstration earthquake early warning system in the Sichuan-Yunnan border region. *Seismological Research Letters*, *91*, 835–846. https://doi.org/10.1785/0220190101

Peng, H. S., Wu, Z. L., Wu, Y.-M., Yu, S. M., Zhang, D. N., & Huang, W. H. (2011). Developing a prototype earthquake early warning system in the Beijing capital region. *Seismological Research Letters*, *82*, 394–403. https://doi.org/10.1785/gssrl.82.3.394

Peresan, A., Zuccolo, E., Vaccari, F., Gorshkov, A., & Panza, G. F. (2011). Neodeterministic seismic hazard and pattern recognition techniques: Time-dependent scenarios for north-eastern Italy. *Pure and Applied Geophysics*, *168*, 583–607. https://doi.org/10.1007/s00024-010-0166-1

Reiter, L. (1990). *Earthquake Hazard analysis: Issues and insights*. Columbia University Press.

Satriano, C., Wu, Y. M., Zollo, A., & Kanamori, H. (2011). Earthquake early warning: Concepts, methods and physical grounds. *Soil Dynamics and Earthquake Engineering*, *31*, 106–118. https://doi.org/10.1016/j.soildyn.2010.07.007

Shi, Y. L., Liu, J., & Zhang, G. M. (2001). An evaluation of Chinese earthquake prediction, 1990-1998. *Journal of Applied Probability*, *38A*, 222–231. https://doi.org/10.1239/jap/1085496604

Wald, D. J., Quitoriano, V., Heaton, H. T., & Kanamori, H. (1999). Relations between peak ground acceleration, peak ground velocity and modified Mercalli intensity in California. *Earthquake Spectra*, *15*, 557–564. https://doi.org/10.1193/1.1586058

Wu, F. T. (1997). The annual earthquake prediction conference in China (National Consultative Meeting on seismic tendency). *Pure and Applied Geophysics*, *149*, 249–264. https://doi.org/10.1007/BF00945170

Wu, Y. M., Chen, D. Y., Lin, T. L., Hsieh, C. Y., Chin, T. L., Chang, W. Y., Li, W. S., & Ker, S. H. (2013). A high-density seismic network for earthquake early warning in Taiwan based on low cost sensors. *Seismological Research Letters*, *84*, 1048–1054. https://doi.org/10.1785/0220130085

Wu, Y. M., & Kanamori, H. (2005). Rapid assessment of damage potential of earthquakes in Taiwan from the beginning of P waves. *Bulletin of the Seismological Society of America*, *95*, 1181–1185. https://doi.org/10.1785/0120040193

Wu, Y. M., Mittal, H., Huang, T. C., Yang, B. M., Jan, J. C., & Chen, S. K. (2019). Performance of low-cost earthquake warning system (P-alert) and shake map production during the 2018 *M*w6.4 Hualien, Taiwan, earthquake. *Seismological Research Letters*, *90*, 19–29. https://doi.org/10.1785/0220180170

Zhang, G. M., Liu, J., & Shi, Y. L. (2002). A scientific evaluation of annual earthquake prediction ability. *Acta Seismological Sinica*, *15*, 550–558.

Zhang, Y., Romanelli, F., Vaccari, F., Peresan, A., Jiang, C. S., Wu, Z. L., Gao, S. H., Kossobokov, G. V., & Panza, G. F. (2021). Seismic Hazard maps based on neo-deterministic seismic hazard assessment for China seismic experimental site and its adjacent areas. *Engineering Geology*, *291*, 10628. https://doi.org/10.1016/j.enggeo.2021.106208

Zhang, Y., Wu, Z. L., Romanelli, F., Vaccari, F., Jiang, C. S., Gao, S. H., Li, J. W., Kossobokov, G. V., & Panza, F. G. (2021). Next-generation EEW combined with NDSHA: From concept to implementation. *Geosciences*, *11*, 473. https://doi.org/10.3390/geosciences11110473

Zhang, Y., Wu, Z. L., Romanelli, F., Vaccari, F., Peresan, A., Zhang, S. F., Jiang, C. S., & Panza, G. F. (2022). Time-dependent seismic hazard assessment based on the annual consultation: A case from the China seismic experimental site (CSES). *Pure and Applied Geophysics*, *179*, 4103–4119. https://doi.org/10.1007/s00024-022-03056-2

Zhu, C. Z., & Wu, Z. L. (2007). Annual consultation on likelihood of earthquakes: Chinese approach to the study and practice of earthquake prediction. In *Secretariat of the organizing committee, the third international conference on continental earthquakes - mechanism, prediction, Emergency Management & Insurance (eds.), collected papers of the third international conference on continental earthquakes* (pp. 486–494). Seismological Press.

How to cite this article: Zhang, Y., Wu, Z., Romanelli, F., Vaccari, F., Peresan, A., Li, J., & Panza, G. F. (2023). Earthquake Early Warning System (EEWS) empowered by Time-Dependent Neo-Deterministic Seismic Hazard Assessment (TD-NDSHA). *Terra Nova*, *35*, 230–239. https://doi.org/10.1111/ter.12647

APPENDIX 1

BLIND ZONE IN THE CASE OF HOMOGENEOUS HALF SPACE

Following Kuyuk and Allen (2013), we consider a simple homogeneous medium with velocities of P- and S-waves V_p and V_s, respectively, and a point source with a focal depth h. The time t_p for the network to 'sense' the earthquake is given by:

$$t_p = T_0 + \frac{R}{V_p} \quad (1)$$

where

$$R = \sqrt{D^2 + h^2} \quad (2)$$

with D being the epicentre distance of the furthest station used for the location and magnitude determination/prediction. The time spent by S-wave to arrive at the target site under consideration is:

$$t_s = \frac{R_0}{V_s} \tag{3}$$

where R_0 is the distance from the seismic source to the target site and D_0 is its epicentre distance:

$$D_0 = \sqrt{R_0^2 - h^2} \tag{4}$$

The condition

$$t_p = t_s \tag{5}$$

determines a threshold epicentre distance Z. When

$$D_0 \leq Z \tag{6}$$

the network 'sense' the earthquake after the arrival of the S-wave, so the early warning is impossible. Thus (6) defines the 'blind zone' of early warning. The radius of such 'blind zone' Z can thus be calculated (Kuyuk & Allen, 2013) as follows:

$$Z = \sqrt{V_S^2 t_p^2 - h^2} \tag{7}$$

APPENDIX 2

PROCEDURE OF THE TD-NDSHA FOR EARTHQUAKE EMERGENCY

The flow chart in Figure A1 describes the procedure of the TD-NDSHA for earthquake emergency, which is adapted from the flow chart of Panza et al. (2022). The main difference lies in two aspects. (1) The 'controlling earthquakes' or 'scenario earthquakes' are from the Annual Consultation, as shown in red; and (2) the result of the ground shaking prediction is mainly used for the identification of the regions of importance for the earthquake early warning system, as shown in blue.

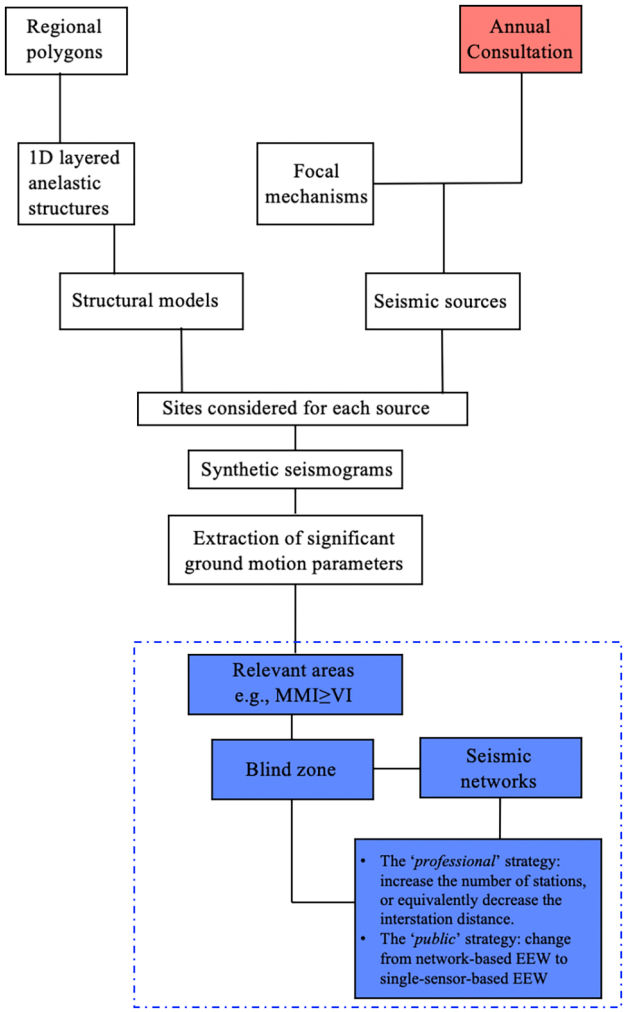

FIGURE A1 Procedure of the TD-NDSHA for earthquake emergency. [Colour figure can be viewed at wileyonlinelibrary.com]